

## ARTICLES

# Structural basis for translation termination on the 70S ribosome

Martin Laurberg<sup>1\*</sup>, Haruichi Asahara<sup>1\*</sup>, Andrei Korostelev<sup>1\*</sup>, Jianyu Zhu<sup>1</sup>, Sergei Trakhanov<sup>1</sup> & Harry F. Noller<sup>1</sup>

**At termination of protein synthesis, type I release factors promote hydrolysis of the peptidyl-transfer RNA linkage in response to recognition of a stop codon. Here we describe the crystal structure of the *Thermus thermophilus* 70S ribosome in complex with the release factor RF1, tRNA and a messenger RNA containing a UAA stop codon, at 3.2 Å resolution. The stop codon is recognized in a pocket formed by conserved elements of RF1, including its PxT recognition motif, and 16S ribosomal RNA. The codon and the 30S subunit A site undergo an induced fit that results in stabilization of a conformation of RF1 that promotes its interaction with the peptidyl transferase centre. Unexpectedly, the main-chain amide group of Gln 230 in the universally conserved GGQ motif of the factor is positioned to contribute directly to peptidyl-tRNA hydrolysis.**

Protein synthesis is carried out by the ribosome, where genetic information encoded in mRNA is translated into a polypeptide chain. Translation ends when a stop codon on mRNA reaches the decoding centre in the A site of the small ribosomal subunit. In contrast to the recognition of sense codons by tRNAs, stop codons are recognized by extra-ribosomal proteins called class I release factors, which also promote hydrolysis of the peptidyl-tRNA linkage in the peptidyl transferase centre of the large ribosomal subunit<sup>1–3</sup>. In bacteria, the UAG and UAA stop codons are recognized by release factor RF1, and the UGA and UAA codons by RF2 (refs 4–6). The low error frequency ( $10^{-3}$ – $10^{-6}$ ) of stop codon recognition is accomplished without a proof-reading mechanism<sup>7</sup>. In principle, stop codons could be recognized directly by specific molecular interactions with the release factors, indirectly by release-factor-promoted interactions with the ribosome, or by some combination of the two. Similarly, hydrolysis of the peptidyl-tRNA linkage could be catalysed by the factors themselves, or by conversion of the ribosomal peptidyl transferase to an esterase by interactions with the factors. Low-resolution cryo-electron microscopy and X-ray studies of termination complexes<sup>8–10</sup> have revealed that the release factors bind to the ribosome in an orientation that roughly coincides with that of a tRNA bound to the A site, placing their extremities in the decoding centre of the small subunit and in the peptidyl transferase centre in the large subunit.

On the basis of mutational studies, a direct recognition model involving a ‘tripeptide anticodon’ has been proposed for stop-codon recognition<sup>11,12</sup>. According to this model, the conserved motifs PxT (in RF1) or SPF (in RF2) decipher the corresponding stop codons. X-ray structures of the release factors bound to the ribosome at 5.9 Å and 6.7 Å resolution<sup>8</sup> showed that these tripeptide motifs are indeed positioned close to the stop codon, but left the mechanism of recognition unresolved. Although structural changes involving the universally conserved nucleotides guanosine (G)530, adenosine (A)1492 and A1493 of 16S have been shown to have a critical role in discrimination of cognate tRNAs<sup>13–15</sup>, it is unclear whether these nucleotides play an active part in translation termination<sup>16,17</sup>.

Mutational analysis and molecular simulation studies have implicated the universally conserved GGQ motif in hydrolysis of the peptidyl-tRNA ester linkage<sup>18–22</sup>. Although its glutamine side chain has been suggested to be involved directly in catalysis<sup>22,23</sup>, mutation of

this residue has generally led to only small effects<sup>19,21,23,24</sup>, whereas mutation of the glycines confers up to  $10^4$ -fold slower rates of peptide release<sup>18,21</sup>. Proposed roles for the GGQ motif include orienting a water molecule for nucleophilic attack<sup>22,23</sup>, passively opening a path for access of a water molecule to the peptidyl transferase centre (PTC)<sup>25</sup> and excluding other nucleophiles from the esterase reaction<sup>21</sup>. Finally, the mechanism by which peptidyl-tRNA hydrolysis is coupled to stop-codon recognition is not understood. Thus, the molecular bases of all three of the principal mechanisms of translation termination remain unresolved.

Here we present the 3.2 Å crystal structure of a translation termination complex containing the *T. thermophilus* 70S ribosome, a defined mRNA, an initiator tRNA<sup>fMet</sup> bound to an AUG codon in the P site, non-cognate tRNA<sup>fMet</sup> in the E site and release factor RF1 bound in response to a UAA stop codon in the A site. The structure reveals that during termination the proline and threonine side chains of the PxT motif both contact the stop codon bases, accompanied by conformational changes in the decoding centre. However, discrimination of the stop codon also involves a network of interactions between the mRNA, 16S rRNA, and backbone and side-chain atoms of RF1 outside the PxT motif. Although Gln 230 of the conserved GGQ motif interacts directly with the PTC, its main-chain amide group, rather than its side chain, is positioned to play a critical part in catalysis. Our structure suggests that stop-codon recognition is coupled to rearrangement of a loop between domains 3 and 4 of RF1, which results in positioning of the GGQ motif in the PTC.

## Recognition of the stop codon

The overall shape and orientation of the release factor in the 70S ribosome (Fig. 1) is similar to that reported in low-resolution X-ray and cryo-electron microscopy studies<sup>8–10</sup>. Domains 2, 3 and 4 of the factor occupy the ribosomal A site, superimposing approximately on the position of tRNA bound to the A site (Fig. 1a, b). The conformations of the decoding centre of the ribosome and of the stop codon in the termination complex differ markedly from those in sense-codon-recognition complexes<sup>14,15</sup> (Supplementary Fig. 2b). In the sense-codon complex, A1492 and A1493 of 16S rRNA both flip out from their ground-state positions in helix 44 (h44) to form A-minor interactions with the minor groove of the codon-anticodon

<sup>1</sup>Department of Molecular, Cell and Developmental Biology and Center for Molecular Biology of RNA, University of California at Santa Cruz, Santa Cruz, California 95064, USA.  
\*These authors contributed equally to this work.

helix (Supplementary Fig. 2b)<sup>14,15</sup>. In the termination complex, only A1492 flips out, leaving A1493 stacked within h44 (Fig. 2a and Supplementary Fig. 2d). A1913, at the tip of the loop of h69 of the 23S rRNA, occupies the space vacated by A1492 in h44 and stacks on A1493 (Fig. 2a and Supplementary Fig. 2d). This conformational change seems to have a critical role in the termination mechanism, as explained later.

The UAA stop codon is bound in a pocket formed by conserved elements of 16S rRNA and domain 2 of RF1, which contains the proposed PxT tripeptide anticodon motif<sup>12</sup> (Fig. 2 and Supplementary Figs 3 and 4). Packing of the tip of helix  $\alpha 5$  of RF1 at Gly 116 against the Watson–Crick edge of uridine (U)1 of the stop codon (Fig. 2b) discriminates against a purine at this position. A hydrogen bond between U1 and the backbone of Gly 116 is possible only with U in this position, as are hydrogen bonds from the Glu 119 backbone amide and the hydroxyl of Thr 186 in the PxT motif to the O4 position of U1. These extensive interactions explain why discrimination is strongest for the first base of the stop codon<sup>7</sup>. In the second position, A2 of the stop codon is stacked between U1 on one side and the imidazole of His 193 on the other. The Watson–Crick edge of A2 packs against the side-chains of Pro 184 and Glu 119; its 6-amino (N6) group hydrogen bonds with the hydroxyl of Thr 186 (Fig. 2b and Supplementary Fig. 4a). Discrimination against guanosine (G) at the second position is probably explained by the inability of its O6 to hydrogen bond with Thr 186 (which donates its only hydrogen to U1). It is less obvious why pyrimidines are excluded here; possible explanations are a weaker propensity for stacking with U1 and the energy penalty caused by a loss of packing against the hydrophobic moieties of Pro 184 and Glu 119. Thus, the PxT motif interacts with the first two bases of the stop codon, rather than with the second and

third bases, as proposed previously<sup>11,12</sup>; however, this motif is by no means the sole determinant of codon recognition.

A3 is unstacked from the first two bases of the stop codon, diverted by the RF1 main chain at residues 192–193 into a position that differs markedly from that of the third base in a sense codon<sup>14,15</sup> (Fig. 2c), stacking instead on G530. Its N6 amino group donates hydrogen bonds to the side chains of Gln 181 and Thr 194, and its N7 accepts a hydrogen bond from the side chain of Thr 194 (Fig. 2c), permitting recognition of both A and G by RF1, while discriminating against pyrimidines. In the backbone of the stop codon, the 2'-hydroxyls of U1 and A2 interact with phosphate 1493 and ribose 1492, respectively, while the 2'-hydroxyl of A3 hydrogen bonds with the main-chain carbonyl of Ile 192 (Fig. 2b, c). Surprisingly, substituting deoxyriboses in the backbone of the stop codon confers only marginal defects in peptide release and RF1 binding<sup>17</sup>, suggesting that these interactions are not critical for stop-codon recognition.

Our structure explains the recently reported observation of competitive binding between RF1 and paromomycin to the ribosome<sup>17</sup>. When paromomycin is bound, A1493 flips out of h44 (ref. 14), sterically preventing the binding of RF1 (Supplementary Fig. 2c); conversely, in the RF1 complex, A1493 occupies the binding site for paromomycin in h44. RF1 function thus involves participation of nucleotides G530, A1492 and A1493, although in an entirely different way from that seen in sense-codon recognition<sup>16,17</sup>. Superposition of the recognition domain of RF2 on that of RF1, on the basis of the similarities in folding of domain 2, and in particular the specificity loops for the structures of the free forms of both type I release factors and of RF1 in the termination complex, allows us to extend our observations to suggest how RF2 may recognize its UAA and UGA codons (see Supplementary Information and Supplementary Fig. 6).

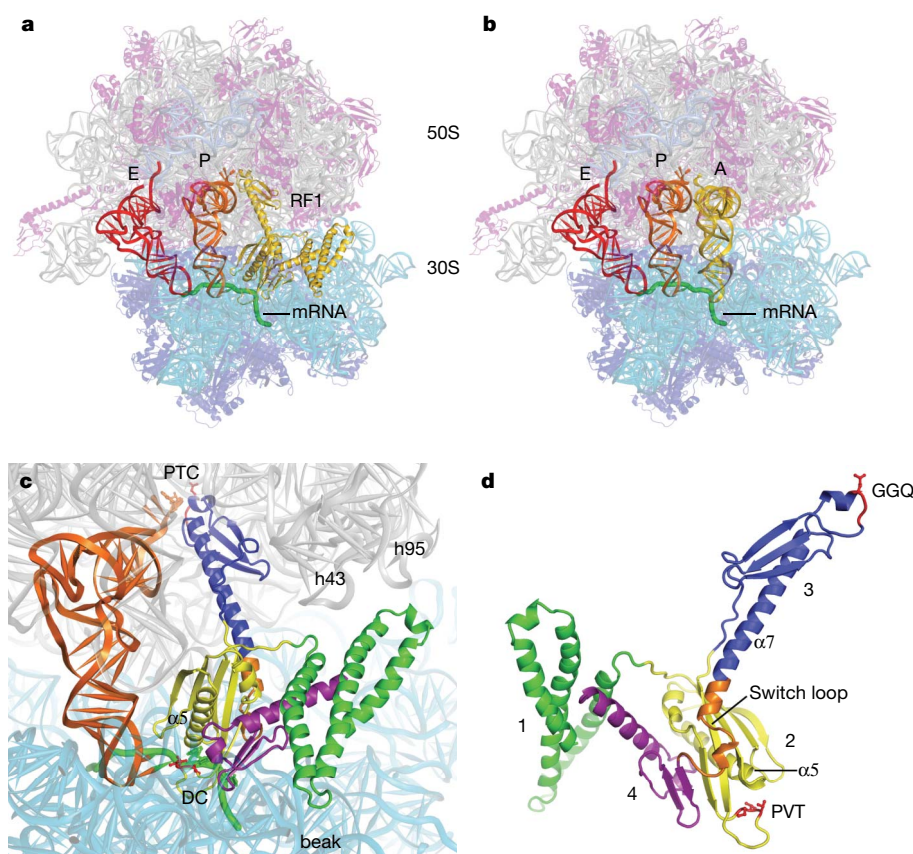


**Figure 1 | Structure of RF1 in the termination complex.** **a**, Positions of RF1 (yellow), P-site tRNA (orange), E-site tRNA (red) and a mRNA (green) in the 70S ribosome. **b**, An elongation complex<sup>43</sup> showing the position of A-site tRNA (yellow) in the context of the current structure. **c**, Orientation of RF1, showing the P-site tRNA (orange), the peptidyl transferase centre (PTC), the

decoding centre (DC) and helices h43 and h95 of 23S rRNA. **d**, The structure of RF1 in its ribosome-bound conformation, rotated  $\sim 180^\circ$  from **a** and **c**. GGQ and PVT motifs are shown in red, and the switch loop (see text) in orange. The domains of RF1 (1–4) are indicated.

### Peptidyl transferase centre

The GGQ motif at positions 228–230, universally conserved in the type I release factors of all organisms, has been implicated in their ability to promote peptidyl-tRNA hydrolysis<sup>18,20</sup>. Biochemical studies have suggested that the role of the factors in the hydrolysis reaction is to convert the ribosomal peptidyl transferase to an esterase in a reaction using water as an acceptor for the peptidyl moiety<sup>2,3,21</sup>. Our structure shows that the GGQ motif indeed resides in the PTC (Fig. 3a), in agreement with previous low-resolution X-ray findings, although the C $\alpha$ -backbone tracing of this region of RF1 as modelled at 5.9 Å resolution<sup>8</sup> is incompatible with the 3.2 Å electron density map. Residues 228–235 rearrange from their free form<sup>26</sup> to form a short helical element (Fig. 3a, b), which probably contributes to the rigidity of placement of the critical residues. At its end, the GGQ motif interacts with the PTC and with A76 of the P-site tRNA (Fig. 3 and Supplementary Fig. 7). The main-chain amide of Gln 230 is found within hydrogen bonding distance of the 3'OH of A76 of the deacylated tRNA bound in the P site (Fig. 3b), whereas its side-chain amide is positioned away from the location of the scissile ester bond, in a pocket formed by A2451, C2452, U2506 and ribose 76 (Fig. 3b and Supplementary Fig. 7), consistent with its proposed role in discrimination of the attacking nucleophile<sup>23</sup>.

The conformations of nucleotides U2506, G2583, U2584, U2585 and A2602 in the PTC of 23S rRNA are consistent with their sensitivity to the occupancies of the A and P sites<sup>15,25,27</sup> (See Supplementary Information and Supplementary Fig. 8f–h). Mutational analysis has shown A2602 to be critical for release-factor-dependent termination<sup>28–30</sup>. Contrary to proposals concerning its

direct involvement in catalysis of the hydrolysis reaction<sup>22,25,29</sup>, A2602 is buried in a cavity in RF1 and blocked from the catalytic site by the path of the main chain of RF1 at Gly 228 (Fig. 4 and Supplementary Fig. 7c). The observed defects in peptide release by A2602 mutant ribosomes<sup>28–30</sup> must therefore be caused by the contribution of A2602 to the binding and/or positioning of domain 3 of RF1 for catalysis.

Proposed mechanisms for the function of RF1 in peptide release include coordination or activation of the attacking water molecule and induction of conformational changes in the PTC<sup>21–23,30</sup>. In our structure, the main-chain amide of Gln 230 is positioned to form a hydrogen bond with the 3'-hydroxyl group of the terminal nucleoside A76 of the deacylated P-site tRNA. Interpretation at this level of structural detail is facilitated by the location of Gln 230 at the end of a helical element, which, supported by the well-resolved electron density for its side chain, places strong constraints on both the position and the orientation of its backbone amide nitrogen (Supplementary Fig. 7b). Thus, the Gln 230 main-chain amide may help to favour ester hydrolysis by coordinating the leaving group (Fig. 3b, c), analogous to a mechanism that has been proposed for hydrolysis of GTP by Ras<sup>31,32</sup>. Moreover, superposition of the structure of a transition-state analogue bound to the 50S subunit<sup>25,33</sup> with our structure places the oxyanion of the transition-state tetrahedral intermediate at hydrogen-bonding distance from the backbone amide nitrogen of Gln 230 (Fig. 3d), suggesting the possibility of transition-state stabilization, and thus potentially contributing to enhancement of the catalytic rate (Fig. 3d, e). When the structure of an oligonucleotide analogue of deacylated tRNA bound at the A site<sup>34</sup> is superimposed on that of the termination complex, the 3'-hydroxyl of its A76 is also

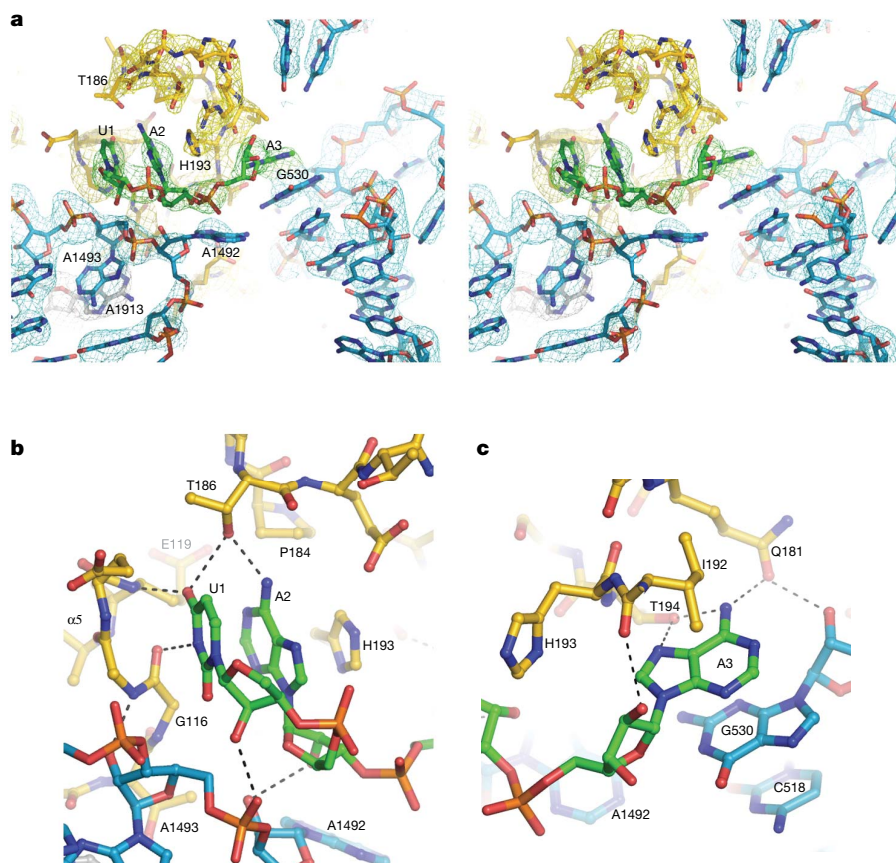


**Figure 2 | Interactions with the UAA stop codon in the decoding centre of the RF1 termination complex.** **a**, Stereo view of  $\sigma_A$ -weighted  $3F_{\text{obs}} - 2F_{\text{calc}}$  electron density map of the stop codon and surrounding elements of the ribosome and RF1. The density for RF1 was contoured at  $1.0\sigma$ , and for the

mRNA and rRNA at  $1.5\sigma$ . **b**, Recognition of U1 and A2 of the UAA stop codon. **c**, Discrimination of the third base (A3) by RF1, showing its stacking on G530 of 16S rRNA. 16S rRNA is shown in cyan, RF1 in yellow, mRNA in green and 23S rRNA (A1913) in grey.

found close to the position of the main-chain amide of Gln 230, although it is positioned less optimally for hydrogen bonding with the 3'-hydroxyl of the P-site A76 or with the transition-state analogue. This could explain why binding of a deacylated tRNA to the A site can catalyse peptide release<sup>2</sup>, albeit at lower rates than the class I release factors<sup>35</sup>. Involvement of the main-chain amide group explains why mutation of Gln 230 has only modest effects on catalysis<sup>19,21,24,36</sup>. Conversely, the absence of a side chain in Gly 229 allows the main-chain amide of Gln 230 to approach the 3'-hydroxyl group of A76 of the P-site tRNA and, similarly, the transition-state intermediate, in keeping with the severe defects in peptide release conferred by mutations in Gly 229 of RF1 (refs 18, 21).

### Communication between the decoding site and the PTC

The danger of premature termination is of critical concern in release factor function. Prevention of hydrolysis of the peptidyl-tRNA linkage before recognition of an authentic stop codon requires strict

coordination of these two events. This is probably accomplished by preventing the final docking of RF1 domain 3 in the PTC until codon recognition is established. In the nearly identical crystal structures of isolated RF1 and RF2 (refs 26, 37), the orientation of domains 2 and 3 differs markedly from that observed in their respective termination complexes<sup>8–10</sup>, indicating a propensity for flexibility in their relative positioning. This is supported by direct observation of both the closed<sup>38</sup> and open<sup>39</sup> conformations of free release factors in solution. Comparison of the ribosome-bound RF1 structure with those of free RF1 or RF2 suggests that a key event involves conformational rearrangement of a loop (residues 286–300) connecting domains 3 and 4, which we term the 'switch loop' (Figs 1d and 5). The result is both to relax its tether on domain 3, allowing it to reach the PTC, and to extend  $\alpha 7$  by two helical turns that are formed from loop residues 286–293 (Fig. 5a). On rearrangement, the switch loop is stabilized by interactions within a pocket formed between the ribosome and RF1 (Fig. 5b). The extra turns of helix formed at the end of  $\alpha 7$  (Fig. 5a) are

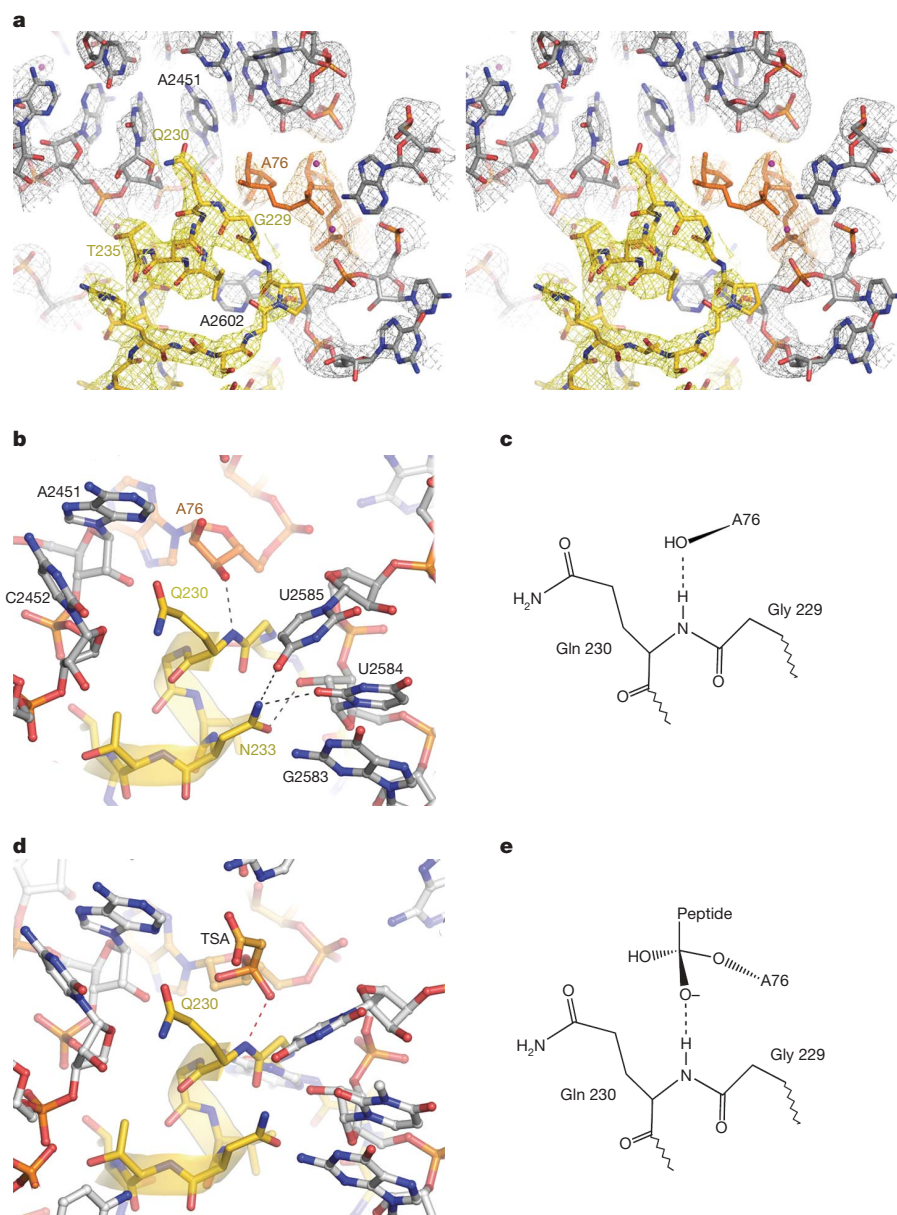


**Figure 3 | Interactions of the GGQ region of RF1 in the PTC.** **a**, Stereo view of  $\sigma_A$ -weighted  $3F_{\text{obs}} - 2F_{\text{calc}}$  electron density for RF1 (yellow), P-site tRNA (orange) and 23S rRNA (grey) contoured at  $1.7\sigma$ . **b**, Position of Gln 230. **c**, Model for product stabilization by hydrogen bonding between the main-chain amide of Gln 230 and the 3'-OH of A76 of the P-site tRNA.

**d**, Superposition of a peptidyl-transferase transition-state analogue (TSA, orange) complexed with the 50S subunit (grey)<sup>25</sup> on the structure of the termination complex (this work). The main-chain amide of Gln 230 is positioned to hydrogen bond with the oxyanion of the TSA. **e**, Model for transition-state stabilization.

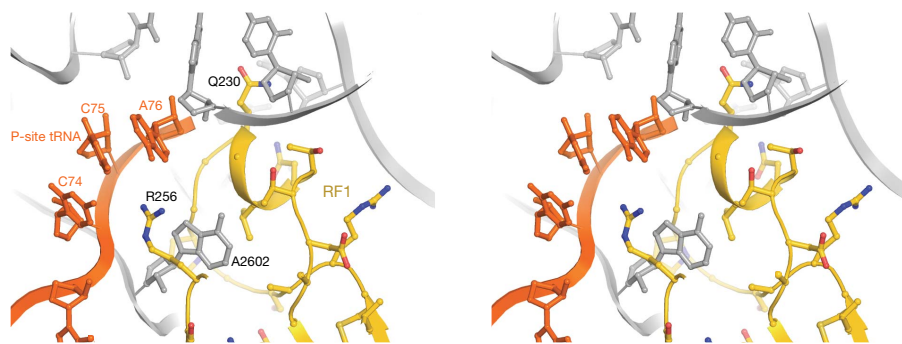


**Figure 4 | Stereo view of the RF1 binding pocket for 23S rRNA nucleotide**

**A2602.** 23S rRNA is shown in grey, P-site tRNA in orange and RF1 in yellow.

held in position by contacts with the  $\beta$ -sheet of domain 2 of RF1 and with residues 1914–1915 in the loop of h69 of 23S rRNA (Fig. 5), directing domain 3 into the PTC.

Rearrangement of the switch loop and positioning of the extended  $\alpha 7$  helix depend on interactions that are made possible by successful stop codon recognition. Flipping out of A1493 or failure of A1913 to stack on A1493 in h44 not only would result in steric clash between these nucleotides and domain 2 of RF1, preventing correct docking of its 'reading head' on the stop codon, but would also affect formation of the binding pocket for the rearranged switch loop and contacts needed to position the extended  $\alpha 7$  helix. Thus, binding of RF1, recognition of the stop codon and the ensuing molecular rearrangements in both the ribosome and the factor leading to docking of the GGQ motif in the PTC are strongly interdependent, cooperative events. The critical interactions involving nucleotides 1913–1915 of 23S rRNA explain the deleterious effects on translation termination caused by deletion of helix 69 of 23S rRNA<sup>40</sup>.

### The mechanism of translation termination

The structure presented here supports the following model for the mechanism of translation termination. The stop codon is bound and recognized in a pocket formed by interactions between the  $\beta$ -sheet of domain 2 of RF1 (including the conserved PxT motif)—the reading head of RF1—and G530, A1492 and A1493—the three critical nucleotides of the 16S rRNA decoding site. A1492 flips out from its position in h44, reminiscent of the events of tRNA selection<sup>14,15</sup>. However, in contrast to the mechanism of sense-codon recognition, A1493 remains stacked within h44, allowing docking of the reading head of RF1 on the stop codon, with which it would otherwise clash. The space vacated by A1492 in h44 is filled by A1913 of 23S rRNA, which stacks on A1493, removing itself and A1493 from a possible clash with RF1. Interactions between RF1 and these rearranged elements of 16S and 23S rRNA induce a conformational change in the switch loop of RF1, which forms an extension of the  $\alpha 7$  helix, creating

a rigid connection between the decoding site and domain 3, docking the latter in the peptidyl transferase centre. Facilitated by product and possibly transition-state stabilization by the main-chain amide group of Gln 230 of RF1, the peptidyl-tRNA linkage is then cleaved. The position of the side chain of the universally conserved Gln 230 is consistent with proposals that it may help to orient the attacking water molecule<sup>22,23</sup> and to discriminate water from other potential nucleophiles<sup>21</sup>, although this would need to be confirmed by the structure of a substrate complex rather than the product complex presented here. An interesting finding is that in the mechanisms of both stop-codon recognition and catalysis, elements of the polypeptide backbone of RF1 seem to have a crucial role. Thus, the basic functions of translation termination could have originated from interactions with simple peptides, possibly as an evolutionary transition from a process that may have initially been carried out by RNA, a possibility supported by the observation that deacylated tRNA bound to the A site is able to catalyse peptide release<sup>2,7,35</sup>.

### METHODS SUMMARY

Ribosomes were purified from *T. thermophilus* HB27, and were then dissociated and reassociated to remove endogenous mRNA and tRNAs as described in Supplementary Methods. A 70S termination complex was formed with RF1, a defined mRNA and tRNAs, and was crystallized essentially as described in ref. 15. The crystal structure was solved by molecular replacement and was refined in CNS<sup>41</sup> and PHENIX<sup>42</sup>, as described.

Received 14 April; accepted 23 May 2008.

Published online 2 July 2008.

1. Capecchi, M. R. Polypeptide chain termination *in vitro*: isolation of a release factor. *Proc. Natl Acad. Sci. USA* **58**, 1144–1151 (1967).
2. Caskey, C. T., Beaudet, A. L., Scolnick, E. M. & Rosman, M. Hydrolysis of fMet-tRNA by peptidyl transferase. *Proc. Natl Acad. Sci. USA* **68**, 3163–3167 (1971).
3. Vogel, Z., Zamir, A. & Elson, D. The possible involvement of peptidyl transferase in the termination step of protein biosynthesis. *Biochemistry* **8**, 5161–5168 (1969).
4. Scolnick, E., Tompkins, R., Caskey, T. & Nirenberg, M. Release factors differing in specificity for terminator codons. *Proc. Natl Acad. Sci. USA* **61**, 768–774 (1968).

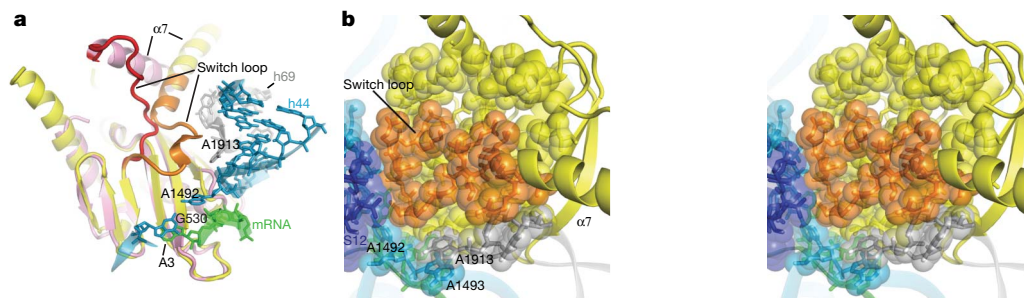


**Figure 5 | Rearrangements and packing of the switch loop of RF1.**

**a**, Superposition of domain 2 of free RF2 (ref. 37; pink) on that of ribosome-bound RF1 (yellow). Rearrangement of the switch loop (red in free RF2 and orange in bound RF1) results in reorientation of  $\alpha 7$  and extension of its length by two helical turns. Free RF2 is shown because of local disorder in the

structure of the otherwise similar free RF1 (ref. 37). **b**, Stereo view of packing of the switch loop (orange) in a pocket formed by elements of protein S12 (dark blue), the  $\beta$ -sheet of domain 2 of RF1 (yellow), the 530 loop of 16S rRNA (cyan) and nucleotides A1492 of 16S rRNA (cyan) and A1913 of 23S rRNA (grey), which form the floor of the pocket.

5. Capecchi, M. R. & Klein, H. A. Characterization of three proteins involved in polypeptide chain termination. *Cold Spring Harb. Symp. Quant. Biol.* **34**, 469–477 (1969).
6. Scolnick, E. M. & Caskey, C. T. Peptide chain termination. V. The role of release factors in mRNA terminator codon recognition. *Proc. Natl Acad. Sci. USA* **64**, 1235–1241 (1969).
7. Freistoffer, D. V., Kwiatkowski, M., Buckingham, R. H. & Ehrenberg, M. The accuracy of codon recognition by polypeptide release factors. *Proc. Natl Acad. Sci. USA* **97**, 2046–2051 (2000).
8. Petry, S. *et al.* Crystal structures of the ribosome in complex with release factors RF1 and RF2 bound to a cognate stop codon. *Cell* **123**, 1255–1266 (2005).
9. Klaholz, B. P. *et al.* Structure of the *Escherichia coli* ribosomal termination complex with release factor 2. *Nature* **421**, 90–94 (2003).
10. Rawat, U. B. *et al.* A cryo-electron microscopic study of ribosome-bound termination factor RF2. *Nature* **421**, 87–90 (2003).
11. Ito, K., Uno, M. & Nakamura, Y. A tripeptide 'anticodon' deciphers stop codons in messenger RNA. *Nature* **403**, 680–684 (2000).
12. Nakamura, Y. & Ito, K. A tripeptide discriminator for stop codon recognition. *FEBS Lett.* **514**, 30–33 (2002).
13. Ogle, J. M., Carter, A. P. & Ramakrishnan, V. Insights into the decoding mechanism from recent ribosome structures. *Trends Biochem. Sci.* **28**, 259–266 (2003).
14. Ogle, J. M. *et al.* Recognition of cognate transfer RNA by the 30S ribosomal subunit. *Science* **292**, 897–902 (2001).
15. Selmer, M. *et al.* Structure of the 70S ribosome complexed with mRNA and tRNA. *Science* **313**, 1935–1942 (2006).
16. Youngman, E. M., Cochella, L., Brunelle, J. L., He, S. & Green, R. Two distinct conformations of the conserved RNA-rich decoding center of the small ribosomal subunit are recognized by tRNAs and release factors. *Cold Spring Harb. Symp. Quant. Biol.* **71**, 545–549 (2006).
17. Youngman, E. M., He, S. L., Nikstad, L. J. & Green, R. Stop codon recognition by release factors induces structural rearrangement of the ribosomal decoding center that is productive for peptide release. *Mol. Cell* **28**, 533–543 (2007).
18. Frolova, L. Y. *et al.* Mutations in the highly conserved GGQ motif of class 1 polypeptide release factors abolish ability of human eRF1 to trigger peptidyl-tRNA hydrolysis. *RNA* **5**, 1014–1020 (1999).
19. Seit-Nebi, A., Frolova, L., Justesen, J. & Kisselev, L. Class-1 translation termination factors: invariant GGQ minidomain is essential for release activity and ribosome binding but not for stop codon recognition. *Nucleic Acids Res.* **29**, 3982–3987 (2001).
20. Mora, L. *et al.* The essential role of the invariant GGQ motif in the function and stability *in vivo* of bacterial release factors RF1 and RF2. *Mol. Microbiol.* **47**, 267–275 (2003).
21. Shaw, J. J. & Green, R. Two distinct components of release factor function uncovered by nucleophile partitioning analysis. *Mol. Cell* **28**, 458–467 (2007).
22. Trobro, S. & Aqvist, J. A model for how ribosomal release factors induce peptidyl-tRNA cleavage in termination of protein synthesis. *Mol. Cell* **27**, 758–766 (2007).
23. Song, H. *et al.* The crystal structure of human eukaryotic release factor eRF1—mechanism of stop codon recognition and peptidyl-tRNA hydrolysis. *Cell* **100**, 311–321 (2000).
24. Seit Nebi, A., Frolova, L., Ivanova, N., Poltarau, A. & Kisselev, L. Mutation of a glutamine residue in the universal tripeptide GGQ in human eRF1 termination factor does not cause complete loss of its activity. *Mol. Biol. (Mosk.)* **34**, 899–900 (2000).
25. Schmeing, T. M., Huang, K. S., Strobel, S. A. & Steitz, T. A. An induced-fit mechanism to promote peptide bond formation and exclude hydrolysis of peptidyl-tRNA. *Nature* **438**, 520–524 (2005).
26. Vestergaard, B. *et al.* Bacterial polypeptide release factor RF2 is structurally distinct from eukaryotic eRF1. *Mol. Cell* **8**, 1375–1382 (2001).
27. Schuwirth, B. S. *et al.* Structures of the bacterial ribosome at 3.5 Å resolution. *Science* **310**, 827–834 (2005).
28. Amort, M. *et al.* An intact ribose moiety at A2602 of 23S rRNA is key to trigger peptidyl-tRNA hydrolysis during translation termination. *Nucleic Acids Res.* **35**, 5130–5140 (2007).
29. Polacek, N. *et al.* The critical role of the universally conserved A2602 of 23S ribosomal RNA in the release of the nascent peptide during translation termination. *Mol. Cell* **11**, 103–112 (2003).
30. Youngman, E. M., Brunelle, J. L., Kochaniak, A. B. & Green, R. The active site of the ribosome is composed of two layers of conserved nucleotides with distinct roles in peptide bond formation and peptide release. *Cell* **117**, 589–599 (2004).
31. Maegley, K. A., Admiraal, S. J. & Herschlag, D. Ras-catalyzed hydrolysis of GTP: A new perspective from model studies. *Proc. Natl Acad. Sci. USA* **93**, 8160–8166 (1996).
32. Li, G. & Zhang, X. C. GTP hydrolysis mechanism of Ras-like GTPases. *J. Mol. Biol.* **340**, 921–932 (2004).
33. Schmeing, T. M., Huang, K. S., Kitchen, D. E., Strobel, S. A. & Steitz, T. A. Structural insights into the roles of water and the 2' hydroxyl of the P site tRNA in the peptidyl transferase reaction. *Mol. Cell* **20**, 437–448 (2005).
34. Schmeing, T. M., Moore, P. B. & Steitz, T. A. Structures of deacylated tRNA mimics bound to the E site of the large ribosomal subunit. *RNA* **9**, 1345–1352 (2003).
35. Zavalov, A. V., Mora, L., Buckingham, R. H. & Ehrenberg, M. Release of peptide promoted by the GGQ motif of class 1 release factors regulates the GTPase activity of RF3. *Mol. Cell* **10**, 789–798 (2002).
36. Dincbas-Renqvist, V. *et al.* A post-translational modification in the GGQ motif of RF2 from *Escherichia coli* stimulates termination of translation. *EMBO J.* **19**, 6900–6907 (2000).
37. Shin, D. H. *et al.* Structural analyses of peptide release factor 1 from *Thermotoga maritima* reveal domain flexibility required for its interaction with the ribosome. *J. Mol. Biol.* **341**, 227–239 (2004).
38. Zoldak, G. *et al.* Release factors 2 from *Escherichia coli* and *Thermus thermophilus*: structural, spectroscopic and microcalorimetric studies. *Nucleic Acids Res.* **35**, 1343–1353 (2007).
39. Vestergaard, B. *et al.* The SAXS solution structure of RF1 differs from its crystal structure and is similar to its ribosome bound cryo-EM structure. *Mol. Cell* **20**, 929–938 (2005).
40. Ali, I. K., Lancaster, L., Feinberg, J., Joseph, S. & Noller, H. F. Deletion of a conserved, central ribosomal intersubunit RNA bridge. *Mol. Cell* **23**, 865–874 (2006).
41. Brunger, A. T. *et al.* Crystallography and NMR system: A new software suite for macromolecular structure determination. *Acta Crystallogr. D* **54**, 905–921 (1998).
42. Adams, P. D. *et al.* PHENIX: building new software for automated crystallographic structure determination. *Acta Crystallogr. D* **58**, 1948–1954 (2002).
43. Yusupov, M. M. *et al.* Crystal structure of the ribosome at 5.5 Å resolution. *Science* **292**, 883–896 (2001).

**Supplementary Information** is linked to the online version of the paper at [www.nature.com/nature](http://www.nature.com/nature).

**Acknowledgements** We thank B. Scott for his input through many stages of this work, and D. Ermolenko, L. Horan, L. Lancaster, B. Scott and D. Staple for comments on the manuscript. We are grateful to the beamline staff at SSRL, ALS and APS for their support during screening and data collection, and to Crystal Chan for her help in using the Berkeley Fermentation Facility. This work was supported by grants from the NIH and NSF (to H.F.N.) and by a fellowship from the Danish Research Council (to M.L.).

**Author Information** Atomic coordinates and structure factors have been deposited with the Protein Data Bank under accession codes 3D5A, 3D5B, 3D5C and 3D5D. Reprints and permissions information is available at [www.nature.com/reprints](http://www.nature.com/reprints). Correspondence and requests for materials should be addressed to H.F.N. ([harry@nuvolari.ucsc.edu](mailto:harry@nuvolari.ucsc.edu)).